Building Simulation 2009

Eleventh International IBPSA Conference
Glasgow, Scotland
July 27-30, 2009

THERMAL MODELING OF THE COOLING CEILING SYSTEMS AS COMMISSIONING TOOL

Nestor Fonseca Diaz[1,2*], Jean Lebrun[2], Philippe André[3]
[1] Universidad Tecnológica de Pereira, Facultad de Ingeniería Mecánica.Colombia.
[2]Thermodinamic Laboratory University of Liège Belgium
Campus du Sart Tilman- Bât: B49 - P33. B-4000 Liège Belgium
[3] Département Sciences et Gestion de l'Environnement, University of Liège Belgium
*Corresponding author:E-mail: nfonseca @utp.edu.co

ABSTRACT

This paper presents the results of a study performed to develop a computational model of cooling ceiling systems. This one has to be used in situ, as diagnosis tool in commissioning process in order to determine the main operating conditions of the system in cooling mode. The model considers the cooling ceiling as a fin. Only the dry regime is considered. From ceiling and room dimensions, material description of the cooling ceiling and measurement of supply water mass flow rate and air and water temperatures, the model calculates the cooling ceiling capacity, ceiling surface average temperature and water exhaust temperature. Fin efficiency, mixed convection close to the cooling ceiling (generated by the ventilation system) and panel perforations influence are studied. A series of experimental results (Laboratory test conditions) got on four types of cooling ceilings are used in order to validate the model.

NOMENCLATURE

A	Area, [m^2]
C	Factor, [-]
c	Specific heat, [J kg^{-1} K^{-1}]
D	Diameter, [m]
h	Superficial (convection and/or radiation) heat transfer coefficient, [W m^{-2} K^{-1}]
k	Thermal conductivity, [W m^{-1} K^{-1}]
L	Length, [m]
$\dot{M}$	Mass flow rate, [kg s^{-1}]
N	Number
NTU	Number of transfer units, [-]
P	Pressure or Perimeter, [Pa] or [m]
$\dot{Q}$	Heat flow, [W]
$\dot{Q}'$	Heat flow per unit length, [W m^{-1}]
q	Heat flow density, [W m^{-2}]
R^l	Thermal resistance per unit length,[m K W^{-1}]
t	Temperature, [°C]
U	Overall heat transfer coefficient, [W m^{-2} K^{-1}]
w	Distance between tubes, [m]
W	Width

Greek symbols

ε	Effectiveness, [-]
δ	Thickness, [m]
ρ	Density or Ceiling panel porosity factor, [kg m^{-3}] or [-]
$\Delta\tau$	Temperature difference, [K]
μ	Dynamic viscosity, [Pa. s]

Subscripts

a	Air
b	Distant between tube axis and ceiling surface
c	Characteristic or cross-sectional
cc	Cooling ceiling
conv	Convective
e	External
ex	Exhaust
exp	Experimental
f	Fictitious , façade or fin
h	Convection
i	Internal
meas	Measured
mr	Mean radiant
p	Panel or panels blocks connected in parallel
rad	Radiative
res	Resultant
su	Supply
s	Panels connected in series or surface
sim	Simulated
t	Tube
w	Water
x	Fin distance
0	Fin base

INTRODUCTION

Thermally active cooling ceilings have been in successful use for many years in commercial applications, with a high percentage of sensible heat removed and low energy consumption. According to Conroy et al. (2005), cooling ceiling systems significantly reduce the amount of air transported through the building (often only about 20% of the normal all-air system air flow rates. This results in the reduction of the fan size, energy consumption and ductwork cross-sectional dimensions (Feustel and Stetiu 1995).

Considering the large surface available for heat exchange, the water temperature is only slightly lower than the room temperature; this small difference allows the use of either heat pump with

very high coefficient of performance (COP), or alternative cooling sources.

Today there is a widespread interest in extending the range of application to heating, in order to save on investment costs on one hand, and on the other one to avoid the use of static heaters under or in front of glass facades, which are often undesirable for architectural reasons.

This article summarizes an experimental investigation and the modeling of two cooling ceiling systems with four different configurations.

DESCRIPTION OF THE STUDIED SYSTEMS

The system is studied here in two constructive versions, used in one and three configurations repectively : Copper tube and synthetic capillary tube mats.

The first constructive version consists of a ceiling in which the copper cooling coils are in direct contact with a smooth perforated metallic surface. The pipe-radiant panel contact must be established in such a way to get a minimum thermal contact resistance; a perforated plate assures suitable convective flow to improve its performance (Figure 1).

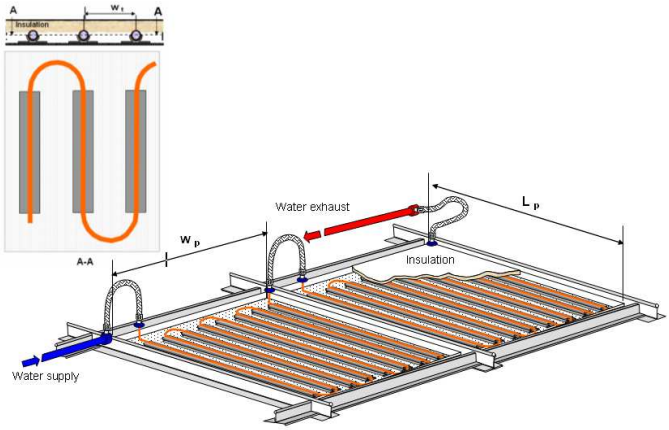

Figure 1: Copper tube cooling ceiling.

The second constructive version uses cooling mats consisting of numerous thin capillary tubes (Di = 2.3 mm) made in polyethylene that are arranged in parallel. The distance between the individual small tubes through which chilled water flows is small enough to ensure that a homogeneous temperature is produced on the bottom side of the ceiling (Figure 2). The cooling mats in this system can be incorporated into the ceiling in three configurations: placed on top of the metal ceiling panels with a layer of mineral wool installed above, embedded into a ceiling plaster layer or stretched between insulation and gypsum plasterboard (Figure 3).

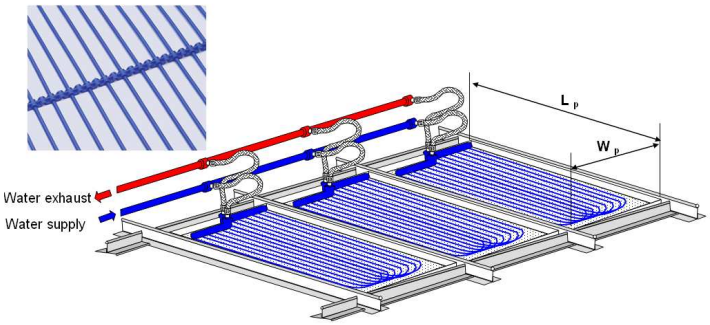

Figure 2 View of Synthetic capillary tube mats cooling ceiling.

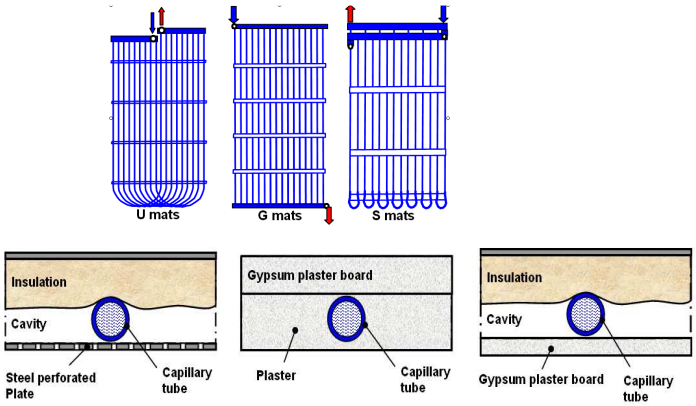

Figure 3 Capillary tube mats configurations and radiant surfaces

The main geometric characteristics of the tested cooling ceiling are summarized in Table 1.

Table 1: Tested cooling ceiling characteristic.

Characteristic	Copper	U mats	S mats	G mats
Radiant surface	On top of a steel plate Thickness 0.8mm	On top of a steel plate Thickness 0.8 mm	Embedded in plaster Thickness 26 mm	On top of gypsum plaster board thickness 10 mm
Panel length L_p	1.15 m	1.37 m.	3.5 m	3.7 m
Panel Width W_p	1.25 m	0.617 m	0.87 m	0.23 m
Tube separation w_t	100 mm.	10 mm.	15 mm	10 mm.
Panel surface	1.44 m^2	0.845 m^2	3.06 m^2	0.85 m^2
Perforated area **ρ**	21 %	16 %	-------	-------
Panels in series N_s	4	1	1	2
Panels in parallel N_p	2	12	4	6
Upward insulation:	30 mm mineral wool.	20 mm mineral wool.	-------	30 mm mineral wool.
Tube-radiant surface union system	Aluminum interconnecti on profile on top of the metal panels	Directly placed on top of the metal panels	Attached below a drywall and then plastered in.	Directly placed on top of the gypsum plasterboards
D_e	13 mm	3.4 mm	3.4 mm	3.4 mm
D_i	12.5 mm	2.3 mm	2.3 mm	2.3 mm

MODEL DESCRIPTION

Copper tube cooling ceiling modeling

An individual element can be defined as shown in Figure 4. Considering the symmetry between tubes, the applicable boundary conditions are:
1) No heat flow in the fin representing the ceiling at midway between the tubes
2) Ceiling fin base temperature (t_{cc0}) and the fin temperature immediately below the tube.

On the axial orientation, a nominal tube length of L_{tp} has to be chosen.

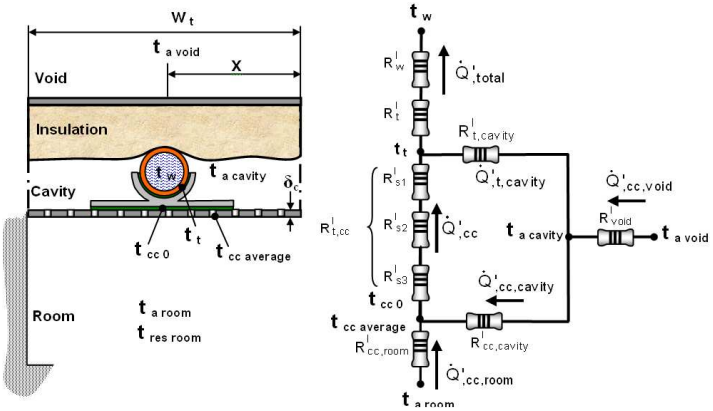

Figure 4: Individual copper tube cooling ceiling element and its equivalent thermal circuit

The following basic assumptions are used in the simulation model:

- Uniform temperature and humidity in the room air.
- Steady-state, one-dimension heat transfer.
- Ceiling panel located in a mechanically ventilated space.
- Transition or turbulent flow inside the tubes (design condition).

The cooling ceiling model can be characterized by the inputs, outputs and parameters shown in Figure 5.

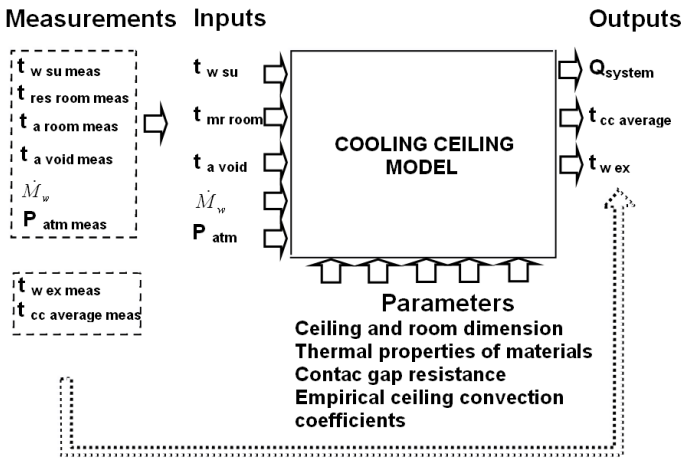

Figure 5: Definition of the cooling ceiling model inputs outputs and parameters

Heat flow definition

According to Figure 4, the total water enthalpy flow rate per unit of length corresponds to the addition of the total thermal energy extracted by the cooling ceiling panel ($\dot{Q}'_{,cc}$) with the heat gain through the tube external surface from the ceiling cavity ($\dot{Q}'_{,t,cavity}$):

$$\dot{Q}'_{,total} = \dot{Q}'_{,cc} + \dot{Q}'_{,t,cavity} \quad [W/m] \quad (1)$$

with:

$$\dot{Q}'_{,total} = \frac{t_{w,average} - t_t}{R'_w + R'_t} \quad [W/m] \quad (2)$$

where:

$$t_{w,average} = \frac{t_{w,su} + t_{w,ex}}{2} \quad [°C] \quad (3)$$

The total heat flow extracted by the cooling ceiling panel ($\dot{Q}'_{,cc}$) corresponds to the sum of the heat flows (convection + radiation) coming from the ceiling cavity ($\dot{Q}'_{,cc,cavity}$) and from the room ($\dot{Q}'_{,cc,room}$) according to:

$$\dot{Q}'_{,cc} = \dot{Q}'_{,cc,room} + \dot{Q}'_{,cc,cavity} \quad [W/m] \quad (4)$$

The cooling ceiling average temperature is one of the outputs of the model; it can be calculated with reference to the fin effectiveness (Eq. 5) (Figure 6).

$$t_{cc,average} = t_{a,cc} - \varepsilon_{fin} \cdot (t_{a,cc} - t_{cc,0}) \quad [°C] \quad (5)$$

The air temperature close to the cooling ceiling surface ($t_{a\,cc}$) is defined as a weighted average of $t_{a,cavity}$ and $t_{a,room}$; the weighting factors are the heat transfer coefficients (Lebrun J. ,2004):

$$t_{a,cc} = \frac{h_{cc,room} \cdot t_{a,room} + h_{cc,cavity} \cdot t_{a,cavity}}{h_{cc,room} + h_{cc,cavity}} \quad [°C] (6)$$

The cooling ceiling heat transfer coefficient can be defined as:

$$h_{cc} = h_{cc,room} + h_{cc,cavity} \quad [W/m^2K] \quad (7)$$

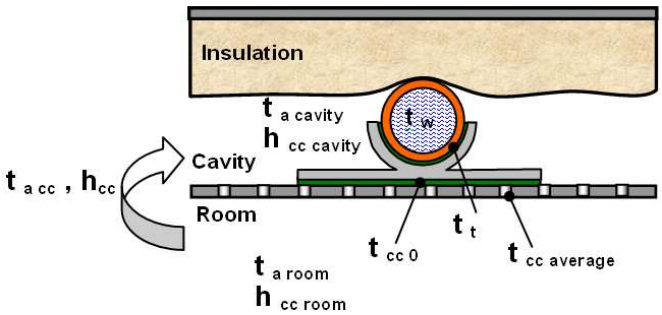

Figure 6: Heat transfer and temperature definition

The temperature distribution along a one-dimensional fin is described by the following equation:

$$\frac{d^2 t_{cc}}{dx^2} = \frac{h_{cc} P}{A_c k_{cc}} \left(t_{cc\,average} - t_{a;cc} \right) \quad (8)$$

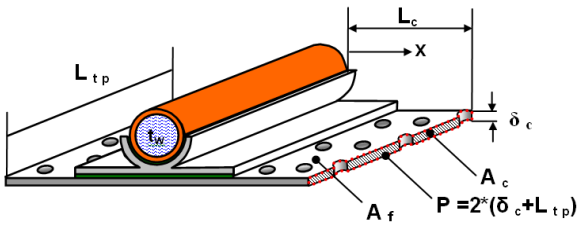

Figure 7: Individual ceiling element as a fin

The solution of this equation gives the following expression for the fin temperature in a section "x":

$$\frac{t_{cc,x} - t_{a,cc}}{t_{cc,0} - t_{a,cc}} = \frac{\cosh(m \cdot (L_c - x))}{\cosh(m \cdot L_c)} \quad (9)$$

with:

$$m^2 = h_{cc} \cdot \frac{P}{A_c \cdot k_{cc}} \quad (10)$$

and:

$$L_c = \frac{w_t - D_e}{2} \quad [m] \quad (11)$$

The effectiveness of this equivalent fin can be defined by Eq (12).

$$\varepsilon_{fin} = \frac{Mf \cdot \tanh(m \cdot L_c)}{h_{cc} \cdot A_f} \quad [-] \quad (12)$$

Where A_f is the surface area of the fin (Figure 7) and:

$$Mf = \sqrt{h_{cc} \cdot P \cdot k_{cc} \cdot A_c} \quad (13)$$

The influence of panel perforation on the fin behavior is too complex to find a fully satisfactory theoretical approach. Only a simplified approach is used here; it's based on the definition of a fin porosity factor **ρ.** The following effects are considered: environmental heat transfer area, heat conduction inside fin and surface temperature.
The fin geometry can be redefined as:

$$P = 2 \cdot \left[\frac{\delta_{cc}}{L_{t,p}} + 1 \right] \cdot (1 + \rho) \quad [-]\text{(Per unit of length)} \quad (14)$$

$$A_c = \delta_c \cdot (1 - \rho) \quad [m]\ \text{(Per unit of length)} \quad (15)$$

$$A_f = P \cdot L_c \cdot (1 - \rho) \quad [m]\ \text{(Per unit of length)} \quad (16)$$

The heat gain from ceiling void through the insulation (Figure 4) can be expressed as a function of the air void temperature (taken as an input in this model) and the void thermal resistance (combination of conduction and convection through the insulation).

Thermal resistance definitions

Water to internal tube surface (R^l_w):

$$R^l_w = \frac{1}{A_w \cdot h_w} \quad [mK/W] \quad (17)$$

The order of magnitude for Re_D with the conditions used for experimental validation of the model is 2168 ~5743 for the copper tubes (and 4108~12214 for the capillary tubes which will be considered later). Therefore the Gnielinski equation (Eq. 18) can be used for forced convection inside tubes in transition or turbulent flow (Celata et al. 2007).

$$Nus_w = \frac{\frac{f_r}{8} \cdot (Re_D - 1{,}000) \cdot Pr_w}{1 + 12.7 \cdot \left[\frac{f_r}{8} \right]^{(1/2)} \cdot (Pr_w^{(2/3)} - 1)} \quad [-] \quad (18)$$

where:

$$fr = (1.82 \cdot \log(Re_D) - 1.64)^{-2} \quad [-] \quad (19)$$

and:

$$Re_D = 4 \cdot \frac{\frac{\dot{M}_w}{N_p}}{\pi \cdot D_i \cdot \mu_w} \quad [-] \quad (20)$$

Tube shell (R^l_t):

$$R^l_t = \frac{\ln\left[\frac{D_e}{D_i} \right]}{2 \cdot \pi \cdot k_t} \quad [mK/W] \quad (21)$$

Cooling ceiling thermal contact resistance (R^l_{tcc}):

The resistance can be divided into 3 parts (Figure 4): contact resistance between tube external surface and interconnection profile (R^l_{s1} bond contact gap1), conductive resistance through the interconnection profile (R^l_{s2}) and contact resistance between interconnection profile and ceiling plate (R^l_{s3} bond contact gap2). Consequently, the total resistance is:

$$R^l_{t,cc} = R^l_{s1} + R^l_{s2} + R^l_{s3} \quad [mK/W] \quad (22)$$

with:

$$R^l_{s1} = \frac{\ln\left[\frac{D_e + 2 \cdot \delta_{s1}}{D_e} \right]}{\pi \cdot k_{s1}} \quad [mK/W] \quad (23)$$

Where δ_{s1} is the bond thickness gap obtained from experimental results (**as a model parameter**). As the interconnection profile's cross section shape and geometry are difficult to evaluate, a fictitious rectangular cross section is defined for the modelling, with base A_{s2} (contact surface) and thickness δ_{s2} :

$$R^l_{s2} = \frac{\delta_{s2}}{A_{s2} \cdot k_{s2}} \quad [mK/W] \quad (24)$$

The net effect of these simplifications on R^{I}_{s2} calculation is relatively small, considering the high thermal conductivity of the interconnection profile (usually made in aluminum). For R^{I}_{s3}, the same methodology is used, but in this case, it is assumed that:

$$R^{I}_{s3} = \frac{\delta_{s3}}{A_{s3} \cdot k_{s3}} \quad \text{[mK/W] (25)}$$

where: $\delta_{s3} = \delta_{s1}$ and $A_{s3} = A_{s2}$.

Ceiling plate thermal resistance (R^{I}_{cc}):

$$R^{I}_{cc,cavity} = \frac{1}{h_{cc,cavity} \cdot A_{cc,cavity}} \quad \text{[mK/W] (26)}$$

$$R^{I}_{cc,room} = \frac{1}{h_{cc,room} \cdot A_{cc,room}} \quad \text{[mK/W] (27)}$$

$A_{cc\ cavity}$ and $A_{cc\ room}$ are the ceiling element surfaces in contact with the air ceiling cavity and room respectively.
A similar methodology is used for the thermal resistance of the tube surface in the ceiling cavity.

Heat transfer coefficient definitions

Between ceiling panel and room ($h_{cc\text{-}room}$):

Both convection and radiation have to be considered:

$$h_{cc,room} = h_{cc,room,conv} + h_{cc,room,rad} \text{[W/m}^2\text{K] (28)}$$

Room-Ceiling convection ($h_{cc\ room\ conv}$):

For the studied element:

$$h_{cc,room,conv} = \frac{k_a}{L_{c,cc}} Nu_{cc,room} \quad \text{[W/m}^2\text{K] (29)}$$

According to what is recommended in ASHRAE System and Equipment Handbook (2004) the following natural convection law can be used here:

$$Nu_{cc,room} = C_{h,cc,room} Ra^{1/n}_{cc,room} \text{ [-]} \quad (30)$$

For pure free convection in a cooled plate facing downwards the coefficient $\mathbf{C_{h,cc,room}=0.54}$ and n=4 (for $10^4 \leq Ra \leq 10^7$) or $\mathbf{C_{h,cc,\ room}=0.15}$ and n=3 (for $10^7 \leq Ra \leq 10^{11}$) (Incropera 1996)**.**
However, among others to make sure that the cooling ceiling system is operates only in dry regime, moisture has usually to be removed from the room through a mechanical ventilation system which generate some air movement.
Because the convective heat transfer is enhanced by both air movement and perforations effects, the use of the natural convection heat transfer coefficient is inappropriate for a mechanically ventilated room. Therefore $C_{h,cc,\ room}$ is considered here as **a model parameter** to be identified on the basis of experimental tests.

The convective heat transfer coefficient of the cooling ceiling $h_{cc.room.conv}$ is currently found in the range of 5.9 ~ 6.5 W/m^{2}K with Ra ≈ 3*10^8 and $\mathbf{C_{h,cc,\ room}}$ **= 0.286**. This actually corresponds to a very strong enhancement by ventilation and perforations effect.

Room-Ceiling radiation ($h_{cc\ room\ rad}$):

Several methods have been developed to simplify the radiation exchange into the room by reducing a multisurface enclosure to a two-surface approximation. In the mean radiant temperature method (MRT) (Walton G.N. 1980), the thermal radiation interchange inside an indoor space is modeled by assuming that the surfaces radiate to a fictitious, finite surface that gives about the same heat flux as the real multisurface case.

When the surface emittances of the enclosure are nearly equal, and the surfaces directly exposed to the cooling ceiling are at the same temperature, the fictitious temperature become the area-weighted average uncooled temperature (AUST) widely used at the related literature (Kilkis 1995, Jeong and Mumma 2004, ASHRAE System and Equipment 2004). For this modeling however, the fictitious temperature considered is the mean radiant temperature. The MRT equation may be written as:

$$\dot{Q}_{cc,room,rad} = A_{cc,efective} \cdot \sigma \cdot F_{r,room} \cdot \left(\left(t_{cc,average} + 273.15 \right)^4 - \left(t_{mr,room} + 273.15 \right)^4 \right)$$

[W] (31)

The mean radiant temperature of the room uncooled surfaces ($t_{mr\ room}$) can be calculated by correcting the mean radiant temperature of the room as the cooled ceiling "sees" an environment which excludes its own influence (Ternoveanu et al. 1999):

$$t_{mr,room} = \left[2 \cdot t_{res,room} - t_{a,room} - \frac{A_{cc,s}}{A_{room,f,s}} \cdot t_{cc,average} \right] \cdot \left[\frac{1}{1 - \frac{A_{cc,s}}{A_{room,f,s}}} \right] \text{[°C] (32)}$$

Eq. (32) is applicable only if: $\left| t_{mr\ room} - t_{a\ room} \right| < 4$ K (Külpmann R.W.1993).
The radiation exchange factor ($F_{r\ room}$) for any two diffuse, gray surfaces that form an enclosure can be expressed by Eq. (33) (Incropera 1996).

$$F_{r,room} = \frac{1}{\frac{1}{F_{cc,f}} + \frac{1}{\varepsilon_{cc}} - 1 + \frac{A_{cc,s}}{A_{room,f,s}} \cdot \left[\frac{1}{\varepsilon_{f,room}} - 1 \right]} \text{[-] (33)}$$

Where:
F_{ccf} : radiation view factor from ceiling to a room fictitious surface giving an equivalent heat transfer, as in the real multi-surface case (1.0 for flat ceiling ASHRAE 2004).

$A_{cc,s}$, $A_{room,f,s}$: area of cooling ceiling and fictitious room surface (other than the ceiling surface).
ε_{cc}, and $\varepsilon_{f\ room}$: emissivities of ceiling and fictitious surface (0.9 and 0.98 respectively (ASHRAE 2005)).
The radiation heat transfer coefficient can be expressed finally as:

$$h_{cc,room,rad} = \sigma \cdot F_{r,room} \cdot \left[\frac{(t_{cc,average} + 273.15)^4 - (t_{mr,room} + 273.15)^4}{t_{cc,average} - t_{a,room}} \right] \quad [W/m^2K] \quad (34)$$

The current order of magnitude found for $h_{c;room;rad}$ using this methodology is 5.25 W/m^{2}K.

A Similar method is used to calculate the heat transfer coefficient on the side of the ceiling cavity.

Global heat transfer characteristics

The total heat flow transferred to the water is calculated as:

$$\dot{Q}_{system} = \dot{Q}'_{,total} \cdot L_{t,p} \cdot \frac{W_p \cdot N_p \cdot N_s}{w_t} \quad [W] \quad (35)$$

Validation process

The AU experimental values can be calculated as:

$$AU_{exp} = \frac{|\dot{Q}_{system}|}{\Delta T;Ln;exp}$$

$$\Delta T;Ln;exp = \left| \frac{t_{w;su} - t_{w;ex;exp}}{\ln\left[\frac{t_{w;su} - t_{res;room;centre}}{t_{w;ex;exp} - t_{res;room;centre}} \right]} \right|$$

The AU experimental values, based on the resultant temperature $t_{res,\ room}$ (globe) measured at the centre of the room are presented in Table 2

Table 2: Experimental and calculated values for copper tube cooling ceiling

1 AU [W/K]	2 AU_{exp} [W/K]	3 $Error_{AU}$ [W/K]	4 $\Delta_{T,Ln}$ [K]	5 $\Delta_{T,Ln,exp}$ [K]	6 $t_{w,ex,exp}$ [°C]	7 $t_{w,ex}$ [°C]	8 $\dot{M}_w$ [kg/s]	9 $t_{a,void}$ [°C]	10 $t_{res,room}$ [°C]	11 $t_{a,room}$ [°C]	12 $t_{cc,average}$ [°C]	13 $t_{w,su}$ [°C]
109	107	-0.9948	9.798	9.78	15.87	15.9	0.0656	22.9	23.9	23.8	16.51	12.05
107.3	105.4	-1.926	9.108	9.17	17.66	17.7	0.0638	24.17	25.1	25.1	18.23	14.04
106.7	109.5	2.778	8.522	8.47	17.03	16.99	0.103	23.97	24.5	24.4	18.04	14.88
105.7	107.2	1.534	7.976	7.93	17.26	17.24	0.0856	23.38	24.1	24	18.03	14.89
106.3	106.8	0.5453	8.052	8.02	18.7	18.76	0.0519	24.24	25	24.9	18.87	14.82
106.3	105.9	-0.4202	7.888	7.91	19.44	19.45	0.0532	25.01	25.6	25.5	19.59	15.68
108.3	107.1	-1.175	9.93	9.95	18.87	18.91	0.0526	24.88	26.6	26.7	19.15	14.03
105.7	105.7	-0.03341	7.651	7.63	19.51	19.53	0.0397	23.97	25	24.9	19.14	14.66
105.8	103.8	-1.992	7.782	7.79	19.41	19.49	0.0405	23.9	25.1	25	19.14	14.64
106	105.6	-0.4397	7.834	7.84	19.4	19.42	0.0394	24.18	25	25	19.03	14.38

The model parameters are identified with the help of the software EES (Klein and Alvarado 2001), by minimization of the error between the measured and simulated AU value and water exhaust temperature.
After minimization of the error, the model parameter δ_{s1} (bond gap thickness) is defined as 0.45mm, and $C_{h,cc,\ room}$ = 0.286 and $C_{h,cc,\ cavity}$ = 0.27. The model results for this condition are also shown in Figures 8 and Table 2.
Figure 8 shows the comparison between measured and simulated results of exhaust water temperature.

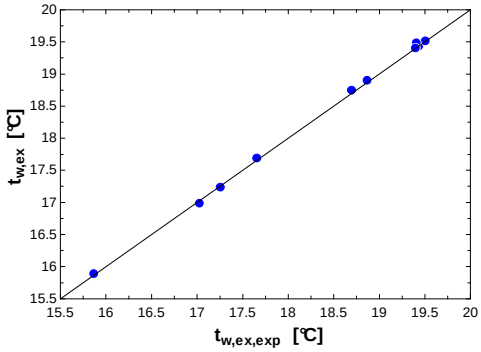

Figure 8: Simulated versus measured exhaust water temperature

The model error is here defined with a method similar to that recommended by the ASHRAE Guideline 2 (2005) for experimental data analysis. By analogy, the average error and the standard deviation are defined as:

$$\bar{\varepsilon} = \frac{1}{n}\sum_{i=1}^{n}\left(V_{i,meas} - V_{i,sim}\right) = \frac{1}{n}\sum_{i=1}^{n}\left(\varepsilon_i\right) \quad (36)$$

$$\sigma = \left[\frac{1}{n}\sum_{i=1}^{n}\left(\varepsilon_i - \bar{\varepsilon}_i\right)^2\right]^{0,5} \quad (37)$$

Where $V_{i,meas}$ is the measured variable and $V_{i,sim}$ is the simulated one.
The model errors are presented in Table 3. The confidence limits are defined by the following equation:

$$\bar{\varepsilon} \pm \frac{Z\sigma}{\sqrt{n}} \quad (38)$$

with a coefficient Z = 1.96 for a probability of 95 %.

Table 3: Copper tubes cooling ceiling model errors.

Variable	Average error	Standard deviation	Minimal deviation	Maximal deviation	Confidence limits
AU [W/K]	-0.21	1.5	-1.53	3.23	1.16 -0.69
$t_{w,ex}$ [K]	- 0.02	0.03	-0.06	0.05	0.008 -0.03

A good agreement is observed between simulated and measured values.
It is also important to observe that, for this type of cooling ceiling, the values obtained for the heat transfer coefficient (forced convection in tubes with diameters 10 mm, h_w =1513 W/m2K) are much bigger than on air side ($h_{cc\ room}$ =11.5 W/m2K). This explains that the AU values presented in Table 2 don't vary very much as function of the mass flow rate.

Synthetic capillary tube mats cooling ceiling

The main geometric characteristics of this configuration are also summarized in Table 1. An

individual element and its equivalent thermal circuit for each tested configuration are shown in Figure 9.

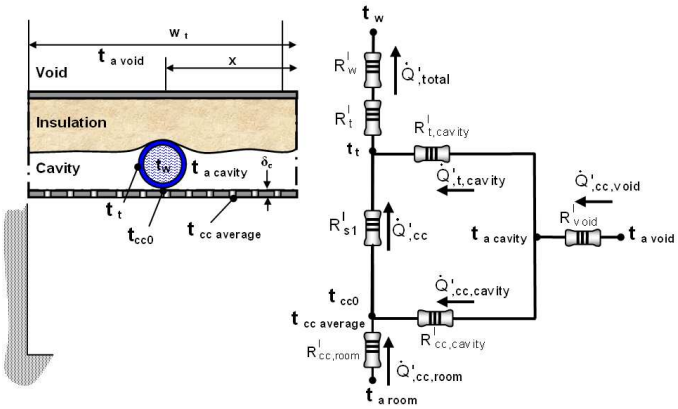

a: Tube mats on top of the metal ceiling panels

b: Tube mats embedded into the ceiling plaster.

c: Tube mats on top of the gypsum plasterboards

Figure 9: Individual synthetic capillary tube mats element and its equivalent thermal circuit

Model description

Almost the same model as the copper cooling ceiling is used, with the following changes only:

- For tube mats on top of the metal panels (Figure 9a), the thermal resistance between the tubes and ceiling plate ($R'_{t,cc}$) is reduced to a fictitious thermal resistance (R'_{s1}) through a reduced air layer of thickness δ_{s1}, which is a **model parameter** to identify on the basis of experimental results.

- For tube mats embedded into the ceiling plaster (Figure 9b), a two-dimensional steady-state conduction heat transfer is considered (the time reaction of this kind of cooling ceiling is less than 15 minutes). The thermal resistance between the tubes and ceiling surface (R^{l}_{s1}) is defined by reference to a horizontal circular cylinder of characteristic length L_{tp}, midway between parallel planes:

$$R^{l}_{s1} = \frac{\ln\left[8 \cdot \frac{b}{\pi \cdot D_e}\right]}{2 \cdot \pi \cdot k_{s1}} \quad \text{[mK/W] (39)}$$

Where **b** value is the distance between tube axis and ceiling surface. This term is a **model parameter** which must be experimentally identified.

- For tube mats on top of the gypsum plasterboards (Figure 9c) there is no air circulation between room and ceiling cavity (plate without perforations, ρ=0).

Validation process

The experimental AU value can be calculated as:

$$AU_{exp} = A_{cc,efective} \cdot U_{exp} \quad \text{[W/K] (40)}$$

$$U_{exp} = \frac{\dot{q}_{exp}}{\Delta_{T,Ln,exp}} \quad \text{[W/m}^2\text{K] (41)}$$

For the tested mats configurations, the cooling ceiling thermal power ($\dot{q}_{exp}$) in W/ m2 is obtained from experimental results according to DIN 4715-1, with constant water mass flow rate and 3 levels of water supply temperature (laboratory reports: FTZ 2003 and HLK Stuttgart University 1995).
The results are shown in Table 4.
Figure 10 shows the comparison between measured and simulated results of exhaust water temperature**.**
It is important to consider that for capillary mats cooling ceilings, the experimental tests were performed without ventilation, according to DIN 4715-1 test condition, therefore, $C_{h\ cc\ room}$ = 0.15 and $C_{h\ cc\ cavity}$ = 0.27 (for Ra=2.5*10^7).
After minimization of the error, the model parameters are: For "**U**" mats configuration δ_{s1}= 0.28mm, for "S" mats b=11.9 mm and for "G" mats δ_{s1}= 0.36mm. The model results for these conditions are shown in Table 4.

Table 4: Experimental and calculated values for synthetic capillary tube mats.

Mats	AU [W/K]	AU_{exp} [W/K]	$Error_{AU}$ [W/K]	$\Delta_{T,Ln,exp}$ [K]	$\Delta_{T,Ln}$ [K]	$t_{w,ex,exp}$ [°C]	$t_{w,ex}$ [°C]	M_w [kg/s]	q_{exp} [W/m2]
U	84.63	84.43	-0.1985	6.251	6.251	20.67	20.67	0.1054	52.2
	87.61	87.7	0.08324	9.085	9.087	17.82	17.82	0.1053	78.8
	90.14	90.2	0.06068	11.77	11.77	16.14	16.14	0.1057	105
S	100.4	100.8	0.3874	12.32	12.31	14.78	14.78	0.1088	101.9
	96.93	96.83	-0.1009	10.01	10.01	16.8	16.81	0.1089	79.6
	96.47	95.76	-0.7013	7.911	7.906	18.68	18.69	0.1091	62.2
G	65.34	64.85	-0.4942	6.724	6.717	19.96	19.97	0.08043	42.7
	66.55	66.65	0.09806	9.086	9.086	17.85	17.85	0.08076	59.3
	68.1	68.55	0.4422	12.13	12.13	15.72	15.72	0.07904	81.4

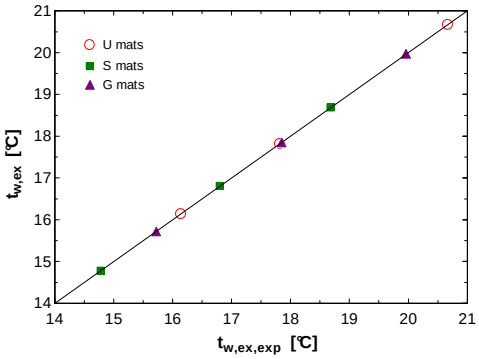

Figure10: Simulated versus measured exhaust water temperature for capillary tube mats cooling ceilings

A very good agreement is observed between simulated and measured values (average difference between simulated and measured AU values and exhaust water temperatures lower than ±0.14 W/K and ±0.003K respectively).

The heat transfer coefficients (forced convection in tubes with diameters of 2.3 mm, h_w = 9341 W/m2K) are much bigger on water side than on air side ($h_{cc, room}$ = 8.8 W/m2K). This makes that, in this case also (and even more), the water flow rate influence on AU value is negligible. But the pressure drop is also important in this case. This makes that pumping energy consumption is no more negligible and can significantly affect the global COP of the cooling system.

CONCLUSIONS

The modeling and experimental validation of four different cooling ceiling systems are presented here as a part of the study of the system in cooling mode. A good agreement is found between simulated and measured values. The theoretical approach gives to the user an appropriate tool for preliminary calculation, design and diagnosis in commissioning processes. The water flow rate has a small influence on cooling ceiling capacity, but the corresponding pressure drop deserves to be carefully checked.

The experimental results show that the convection heat transfer on cooling ceiling surface can be strongly enhanced by action of the auxiliary ventilation system (normally used with this kind of systems).

REFERENCES

ASHRAE HANDBOOK-HVAC Systems and Equipment. 2004. Chapter 6. Atlanta: American Society of Heating, Air-Conditioning and Refrigeration Engineers, Inc.

ASHRAE HANDBOOK. 2005. Fundamentals Atlanta: American Society of Heating, Air-Conditioning and Refrigeration Engineers, Inc.

ASHRAE Guideline 2-2005. Engineering analysis of experimental data. American Society of Heating, Refrigerating, and Air-Conditioning Engineers, Inc., Atlanta, USA.

Celata P., Cumo M and McPhail J., G Zummo. 2007. Single-phase laminar and turbulent heat transfer in smooth and rough microtubes. Microfluid Nanofluids.Vol 3. p.p 697-707.

Conroy C. and Mumma S. 2005. Ceiling Radiant Cooling Panels as a viable distributed Parallel Sensible Cooling Technology integrated with dedicated Outdoor air Systems. ASHRAE tarnsactions, 107. Part 1 AT-01-7-5.

DIN 4715. 1993. Entwurf, Raumkühlflächen; Leistungmessung bei freier Strömung; Prüfregeln, Beuth Verlag GmbH, Berlin.

FTZ Forschungs-und Transferzentrum e.V and der Westsächsischen Hochschule Zwickau (FH). 1995, 2002, and 2003. Prüfbericht über die Ermittung der Kühlleistung einer Raumkühfläche Messung analog DIN 4715-1.

Feustel H. and Stetiu C. 1995. Hydronic radiant cooling- preliminary assessment. Energy and Building.Vol 22. p.p. 193-205.

HLK Heizung Lüftung Klimatechnik Prüfstelle. University of Stuttgar. 1995. Prüfbericht über die Ermittung der Kühlleistung einer Raumkühfläche nach DIN 4715-1. Prüfberich Nr.:VR95 K29. 1134.

Incropera F. and DeWitt D. 1996. Fundamentals of Heat and Mass Transfer. Fourth Edition. School of Mechanical Engineering Purdue University.

Jae-Weon Jeong and Mumma S. 2004. Simplified cooling capacity estimation model for top insulated metal ceiling radiant cooling panels. Applied Thermal Engineering. Vol.24 p.p 2055-2072.

Kilkis B. 1995. Coolp: A computed program for the design and analysis of ceiling cooling panles. ASHRAE Transaction: Symposia. SD 95-4-4. p.p 705-710.

Kulpmann R. 1993 Thermal comfort and air quality in rooms with cooled ceilings – results of scientific investigations; ASHRAE Transactions: Symposia – DE 93 – 2 – 2; p.p 488-502.

Lebrun J. 2004. Climatisation: Transferts de Chaleur et de Masse. Notes de curs. Laboratoire de thermodynamique applique Université de Liège.

Ternoveanu A, Hannay, C, Qingping, W. 1999. Preliminary Analysis on a Research Project for Cooling Ceilings - synthesis of available information. Laboratoire de thermodynamique applique Université de Liège. Belgium.

Walton G.1980. A new algorithm for radiant interchange in room loads calculations. ASHRAE Transaction: 86 (2) 190-208.